Molecular Therapy
Methods & Clinical Development
Original Article

Point Mutations in Retargeted gD Eliminate the Sensitivity of EGFR/EGFRvIII-Targeted HSV to Key Neutralizing Antibodies

Ceren Tuzmen,[1] Tina M. Cairns,[2] Doina Atanasiu,[2] Huan Lou,[2] Wan Ting Saw,[2] Bonnie L. Hall,[1] Justus B. Cohen,[1] Gary H. Cohen,[2] and Joseph C. Glorioso[1]

[1]Department of Microbiology and Molecular Genetics, University of Pittsburgh, Pittsburgh, PA 15219, USA; [2]Department of Microbiology, School of Dental Medicine, University of Pennsylvania, Philadelphia, PA, USA

Effective oncolytic virotherapy may require systemic delivery, tumor targeting, and resistance to virus-neutralizing (VN) antibodies. Since herpes simplex virus (HSV) glycoprotein D (gD) is the viral attachment/entry protein and predominant VN target, we examined the impact of gD retargeting alone and in combination with alterations in dominant VN epitopes on virus susceptibility to VN antibodies. We compared the binding of a panel of anti-gD monoclonal antibodies (mAbs) that mimic antibody specificities in human HSV-immune sera to the purified ectodomains of wild-type and retargeted gD, revealing the retention of two prominent epitopes. Substitution of a key residue in each epitope, separately and together, revealed that both substitutions (1) blocked retargeted gD recognition by mAbs to the respective epitopes, and, in combination, caused a global reduction in mAb binding; (2) protected against fusion inhibition by VN mAbs reactive with each epitope in virus-free cell-cell fusion assays; and (3) increased the resistance of retargeted HSV-1 to these VN mAbs. Although the combined modifications of retargeted gD allowed bona fide retargeting, incorporation into virions was partially compromised. Our results indicate that stacking of epitope mutations can additively block retargeted gD recognition by VN antibodies but also that improvements in gD incorporation into virus particles may be required.

INTRODUCTION

Oncolytic herpes simplex viruses (oHSVs) are among the most widely studied vectors for the treatment of solid tumors. Currently, the only US Food and Drug Administration (FDA)-approved oncolytic virus (OV) is talimogene laherparepvec (T-VEC; Imlygic), an oHSV developed by BioVex (under the name Oncovex^{GM-CSF}) and Amgen for the treatment of metastatic melanoma.[1,2] T-Vec requires intratumoral injections to treat malignant lesions, and its efficacy against metastatic tumors relies on its ability to induce a systemic anti-tumor immune response (abscopal effect). However, this effect can be inadequate against late-stage metastatic disease and so-called "cold" tumors that display a paucity of recognizable neoantigens. In these instances, direct OV infection of metastatic tumors may improve treatment outcome. To this end, development of oHSV that can be systemically administered to selectively infect and replicate in tumors throughout the body and is resistant to pre-existing virus-neutralizing (VN) antibodies would be a breakthrough in metastatic cancer therapy. Therefore, in this study we explored the feasibility of creating "stealth" oHSV that escapes inactivation by pre-existing antibodies and selectively targets primary and metastatic tumor cells while retaining efficient infectivity.

Four viral glycoproteins are necessary for HSV entry into host cells: gD, gB, and the heterodimer gH/gL. The current model of HSV entry involves a stepwise process whereby gD binds to one of its cellular receptors (nectin-1, herpesvirus entry mediator [HVEM], or 3-*O*-sulfotransferase modified heparan sulfate), resulting in a gD-initiated cascade of conformational changes that promote conversion of gB into a fusogenic state through an intermediate interaction with gH/gL.[3,4] This signaling cascade enables fusion of the viral envelope with cell-surface or endosomal membranes and release of the de-enveloped virus particle into the cytoplasm. Since binding of gD to one of its specific receptors initiates the infection process, gD is considered the major determinant of the HSV tropism.

We previously modified gD of HSV-1 to restrict infection to cells expressing a specific non-HSV receptor. Retargeting of HSV requires both removal of gD binding sites for its cognate receptors and introduction of a binding partner for the target receptor of choice. We succeeded in retargeting the virus by (1) substitution of N-terminal gD residues 2–24 with a single-chain variable fragment (scFv) antibody specific for human epidermal growth factor receptor (EGFR) and oncogenic EGFRvIII, abolishing HVEM-binding activity while providing a targeting ligand (Figure 1A); and (2) a point mutation at residue 38 to eliminate nectin-1 binding. As the retargeted viruses showed relatively low infectivity, the modifications in gD were

Received 9 October 2019; accepted 26 December 2019;
https://doi.org/10.1016/j.omtm.2019.12.013.

Correspondence: Joseph C. Glorioso, Department of Microbiology and Molecular Genetics, University of Pittsburgh, School of Medicine, 428 Bridgeside Point II, 450 Technology Drive, Pittsburgh, PA 15219, USA.
E-mail: glorioso@pitt.edu

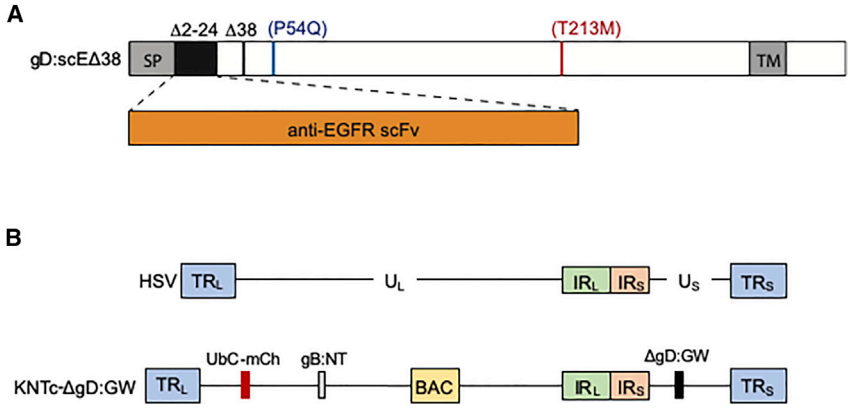

Figure 1. Retargeted gD and Viral Backbone Structures

(A) Retargeted gD (gD:scEΔ38). The black box indicates replacement of residues 2–24 with anti-EGFR scFv (orange box); blue and red vertical bars represent the positions of *mar* mutations P54Q (blue) and T213M (red) introduced individually and in combination into gD:scEΔ38. SP, gD signal peptide; TM, transmembrane domain; Δ38, deletion of gD residue 38. (B) Genome structures of WT HSV (upper) and gD-deficient recombinant KNTc-ΔgD:GW (lower). KNTc-ΔgD:GW contains bacterial artificial chromosome (BAC) sequences between U_L37 and U_L38 for viral genome propagation and engineering in *E. coli*, a ubiquitin C promoter-mCherry expression cassette (UbC-mCh) between U_L3 and U_L4, two viral entry-enhancing mutations in the gB gene (gB:NT), and a GW recombination cassette in place of the gD coding sequence (ΔgD:GW) to allow rapid, orientation-specific insertion of altered gD genes under control of the gD promoter. U_L, unique long segment; U_S, unique short segment; TR_L, terminal inverted repeat flanking U_L; IR_L, internal inverted repeat flanking U_L; TR_S, terminal inverted repeat flanking U_S; IR_S, internal inverted repeat flanking U_S.

coupled with two entry-enhancing mutations in gB, D285N/A549T, referred to as gB:NT (Figure 1B). Retargeted gB:NT viruses exhibited 100-fold increased entry efficiency with infectivity comparable to that of wild-type (WT) gD virus through the canonical HSV-1 entry receptors.[5,6] Together, these modifications eliminated virus toxicity in mouse brain and enabled homing of systemically delivered virus to EGFRvIII-expressing glioma flank tumors in nude mice.[5] The retargeted gD used in our current study (gD:scEΔ38; Figure 1A) includes a deletion of residue 38,[7] instead of the previous point mutation (Y38C), to irreversibly eliminate binding to nectin-1.

Analyses of the antibody responses across multiple human patients exposed to HSV-1 and/or HSV-2 revealed prominent glycoprotein epitopes of WT HSV for VN monoclonal antibodies (mAbs).[8,9] These epitopes can be eliminated by mutagenesis or spontaneous mutation to create mAb-resistant (*mar*) variants.[10] It was demonstrated that HSV neutralization by different human HSV antisera was primarily due to antibodies against either (1) both gD and gB, (2) gD alone, or (3) gB alone.[8,9] We therefore set out to reduce the susceptibility of our retargeted virus initially to gD-specific VN antibodies by identification and rational point mutagenesis of VN mAb epitopes that were preserved in retargeted gD. Using high-throughput, array-based surface plasmon resonance imaging (SPRi) analysis with a collection of 39 gD1-reactive mAbs and soluble gD, we recently showed that these mAbs can be clustered into "communities" or groups recognizing the same or overlapping epitopes on the basis of cross-competition for gD binding, providing insight into the overall antigenic structure of gD.[11] Epitope mapping along with structural analyses created color-coded community maps consisting of (1) yellow and red groups of VN mAbs that block receptor binding, (2) green and blue group mAbs that interfere with the fusion-signaling cascade, and (3) a brown group of predominantly non-neutralizing mAbs that bind to epitopes near the transmembrane domain.[11] Human immune sera compete for gD binding with many of the VN mAbs in this collection,[8,12] suggesting that this collection provides a significant representation of the anti-gD antibody repertoire in these sera. Therefore, removal of gD epitopes recognized by VN mAbs can be expected to reduce virus neutralization by sera from HSV-exposed individuals.

In this study, we used SPRi to identify shared epitopes between WT and retargeted gD as likely VN mAb targets in retargeted oHSV. We selected two gD mutations previously shown to protect WT virus from inactivation by VN mAbs MC5 (P54Q) and MC23 (T213M).[13] These mAbs are representative of those in the blue and red groups, respectively, each neutralizes virus at a different step in the entry pathway, and competition studies suggest that their epitopes are recognized by sera from HSV-exposed individuals.[8,9] We validated these mutations in retargeted gD, both individually and in combination, by measuring (1) mAb binding to purified, soluble retargeted gD proteins via SPRi analysis, (2) fusion activities of full-length retargeted gD proteins *in vitro*, and (3) neutralization susceptibility of retargeted viruses bearing one or both mutations. Additionally, we investigated the effects of the mutations on retargeted gD incorporation into virus envelopes. This is the first study that attempts to evaluate the impact of antigenically altering retargeted gD on the biological activity of the mutated glycoprotein. The results demonstrate that while this strategy for antigenic stealthing may prove feasible, a more thorough mutagenesis and retargeting strategy will be required to overcome loss of gD functional activity.

RESULTS

Retargeting Induces Changes in the Antigenic Structure of gD

We used SPRi analyses of purified gD ectodomains to compare the epitope landscapes of WT and retargeted gD. Ectodomains truncated after gD residue 306 were expressed in a baculovirus system, affinity-purified with anti-gD mAb DL6, and equal amounts of purified proteins were used for SPRi analysis. No binding to retargeted gD was observed for any of the yellow group mAbs (Figure 2A). This was expected since these mAbs recognize the HVEM-binding N-terminal segment of WT gD[11] that is largely replaced with our anti-EGFR/EGFRvIII scFv in the retargeted gD. In addition, we observed decreased binding of mAbs of the green community, and some

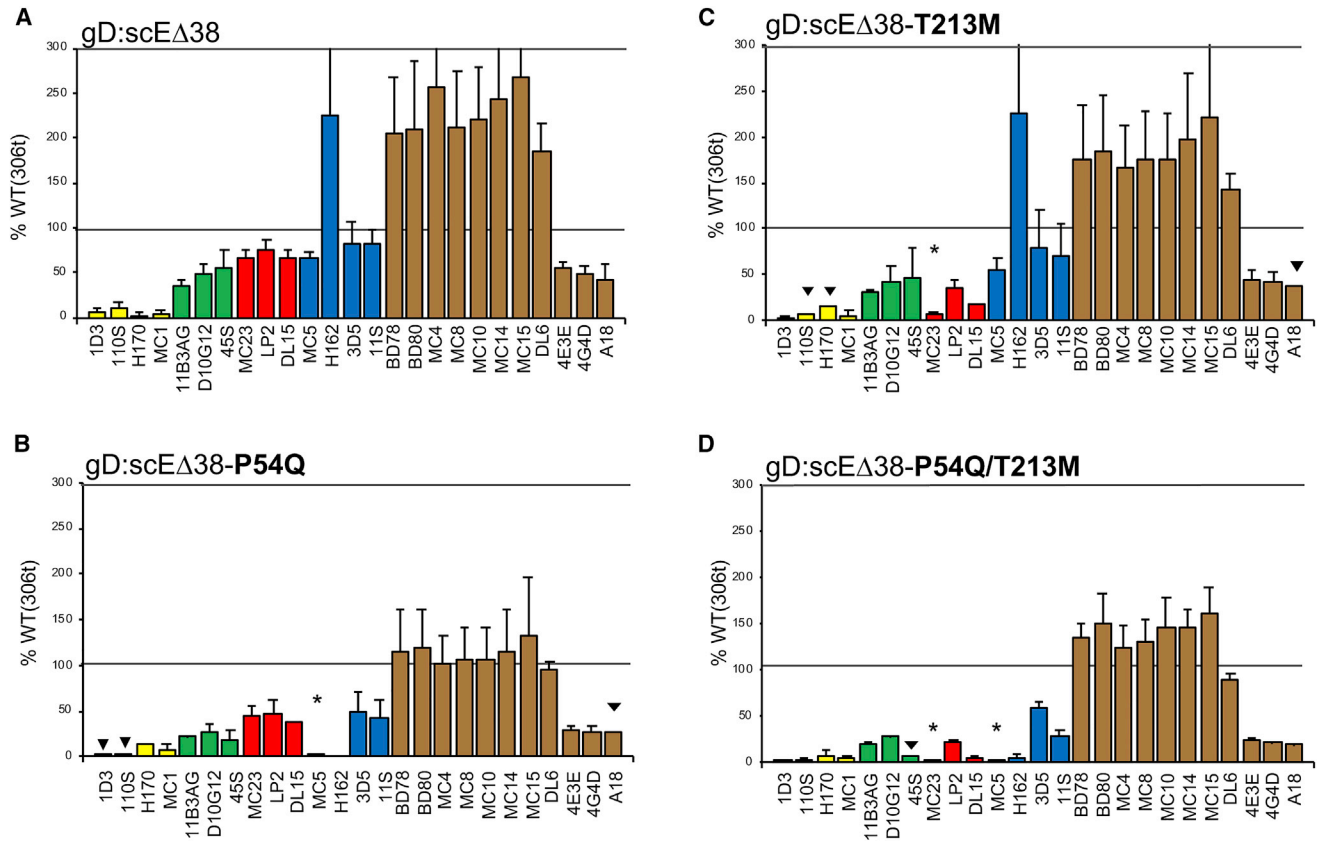

Figure 2. Effects of Retargeting and *mar* Mutations on mAb Binding to Purified gD Ectodomains

The ectodomains of gD:scEΔ38 and its *mar* mutants were expressed in insect cells and purified on an anti-gD (mAb DL6) column. SPRi was used to determine the binding of 25 gD-specific mAbs to each purified protein. (A–D) Representative results show the binding of each mAb to (A) gD:scEΔ38, (B) gD:scEΔ38-P54Q, (C) gD:scEΔ38-T213M, and (D) gD:scEΔ38-P54Q/T213M as a percentage of their binding to the purified soluble ectodomain (306t) of WT gD (100%). Values are averages ± SEM of two or three independent determinations. Black triangles denote a single determination. Statistically significant differences between each gD mutant protein and the parental retargeted protein for each mAb were identified by one-way ANOVA (*$p < 0.01$). mAbs are named below the horizontal axes and grouped according to their designated community (yellow, green, red, blue, or brown).[11]

reduction among mAbs from the red and blue groups. Interestingly, the majority of mAbs in the brown group showed increased binding; these mAbs recognize overlapping linear epitopes in the C terminus of the gD ectodomain and differ from all others in that they do not neutralize WT HSV-1, although they block virus-free cell-cell fusion and lateral virus spread.[11] The remaining mAbs in the brown community (4E3E, 4G4D, A18), distinct from the others in that they bind to conformational epitopes and are neutralizing,[11] showed decreased binding to retargeted gD. These observations indicated that the retargeting modifications measurably affected the conformation of gD.

mar Mutations Further Change the Antigenic Structure of Retargeted gD and Reduce the Binding of Specific Neutralizing mAbs

In order to eliminate the binding of neutralizing mAbs, we created substitution mutations P54Q and T213M in retargeted gD. These *mar* mutations were previously shown to eliminate the binding of VN antibodies MC5 (blue) and MC23 (red), respectively, to WT gD.[14] Of note, human immune sera do not compete with any of the brown mAbs for binding to WT gD, suggesting that the target epitopes of these mAbs may be inaccessible in complete virions and are therefore not recognized by the human humoral immune system. Accordingly, our current effort focused on protection against members of other mAb communities regardless of the potential of brown mAbs to neutralize retargeted HSV. Based on SPRi results, P54Q in retargeted gD (Figure 2B) completely abolished the binding of MC5 and another member of the blue community of mAbs, H162, that had shown increased binding to parental retargeted gD (Figure 2A). This mutation also decreased the binding of two other blue mAbs as well as of the green and brown mAbs, but less dramatically (Figure 2B). T213M appeared to have a more specific effect, causing mildly to severely impaired binding of the red mAbs, MC23 in particular, but no major changes in the binding of other mAbs (Figure 2C). Combining the two mutations in retargeted gD (P54Q/T213M) suggested an additive effect, closely resembling the binding profile of

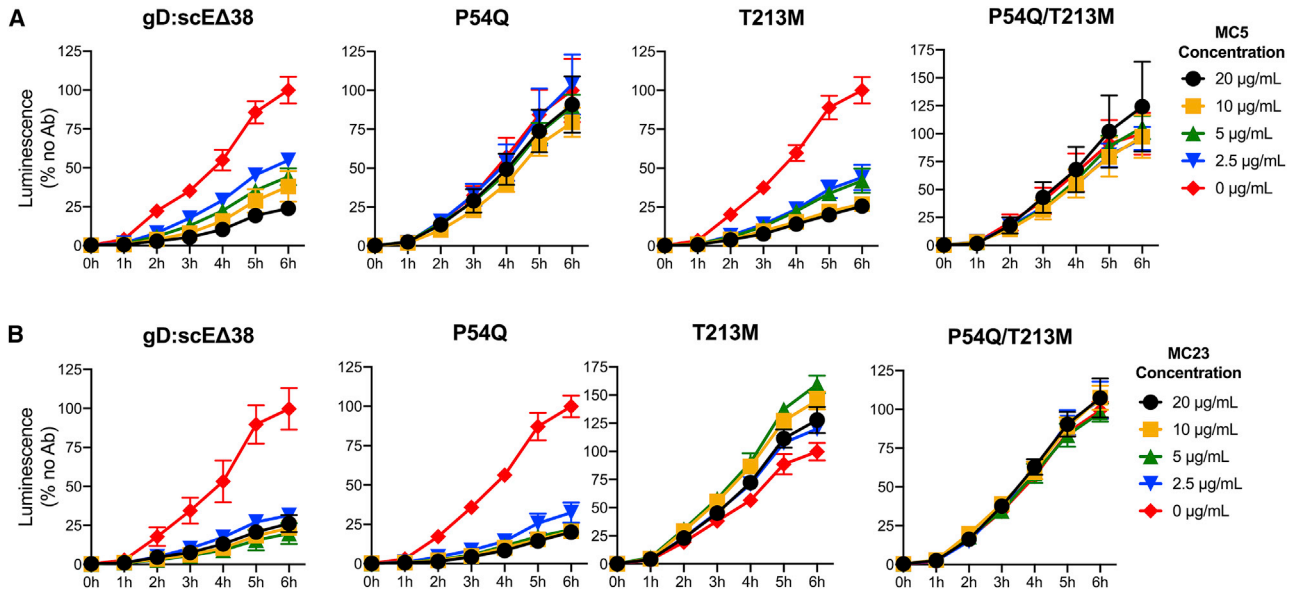

Figure 3. gD Activity in Virus-Free Fusion Assays and Inhibition by mAbs

(A) Inhibition of fusion by mAb MC5. (B) Inhibition by mAb MC23. B78H1 cells were transfected with expression plasmids for gB:NT, gH, gL, different versions of gD, as indicated, and split luciferase N-terminal plasmid $RLuc8_{1–7}$. EGFRvIII-expressing B78-vIII cells were transfected with split luciferase C-terminal plasmid $RLuc8_{8–11}$. Upon mixing of the cells, luminescence resulting from fusion between the two cell populations was measured over time. Antibody inhibition was performed by incubation of the transfected B78H1 cell populations with MC5 or MC23 mAb at the indicated concentrations for 1 h prior to mixing with B78-vIII cells. Data are shown relative to no antibody (red in all graphs) at 6 h (100%). Two independent experiments were performed, each in triplicate. Curves from a representative experiment are shown (averages ± SEM). For each retargeted gD protein, two-way ANOVA was used to identify statistically significant differences in fusion during the 6-h time course at each mAb concentration compared to the no antibody control. For MC5 (A), the fusion activity of the parental gD:scEΔ38 protein was significantly inhibited at 5 ($p < 0.05$), 10 ($p < 0.01$), and 20 μg/mL ($p < 0.01$) and the T213M mutant was inhibited at 2.5 ($p < 0.05$), 5 ($p < 0.05$), 10 ($p < 0.01$), and 20 μg/mL ($p < 0.01$). In contrast, the P54Q and T213M/P54Q mutants were not significantly impaired at any MC5 concentration. For MC23 (B), the activity of the parental gD:scEΔ38 protein was significantly inhibited at 2.5 ($p < 0.05$), 5 ($p < 0.01$), 10 ($p < 0.01$), and 20 μg/mL ($p < 0.01$), and the P54Q mutant was inhibited at all MC23 concentrations ($p < 0.01$). The activities of the T213M and T213M/P54Q mutants were not significantly reduced at any MC23 concentration.

P54Q alone but with limited binding of red mAbs (Figure 2D). Collectively, these results indicated that retargeting combined with single or double *mar* mutations can broadly reduce the antibody recognition of gD.

mar Mutations Block the Ability of Site-Specific mAbs to Inhibit Cell Fusion

We used an *in vitro* fusion assay to determine the sensitivity of retargeted gD function to mAbs MC5 and MC23. HSV entry-receptor-deficient mouse melanoma B78H1 cells were co-transfected with plasmids expressing gB:NT, gH/gL, and full-length retargeted gD, incubated 2 days later with increasing concentrations of either mAb for 1 h, and mixed with EGFRvIII-transduced B78H1 cells (B78-vIII, Figure S1). Fusion between the two cell populations was measured by a split-luciferase assay[15] at 1-h intervals during a period of 6 h. We observed that the fusion activity of cells transfected with the parental retargeted gD construct (gD:scEΔ38) was inhibited in a dose-dependent manner by both MC5 and MC23 (Figure 3). However, the P54Q and T213M mutations completely blocked the inhibitory effects of MC5 (Figure 3A) and MC23 (Figure 3B), respectively, as indicated by the similarity of the fusion curves in both cases for no antibody and all of the antibody concentrations tested. Notably, the P54Q mutant protein remained sensitive to the blocking activity of MC23 (Figure 3B) and the T213M mutant remained sensitive to the blocking activity of MC5 (Figure 3A), while the combined changes (P54Q/T213M) eliminated fusion sensitivity to both mAbs. These observations were consistent with the results of Figure 2 and encouraged examination of the protective potential of the two mutations in the context of retargeted virus.

Virus Construction, Growth, and Entry Specificities

Recombinant viruses expressing parental retargeted gD or its single- or double-mutant derivatives were created as described in Materials and Methods (Figure 1B). Viruses were grown on Vero cells that naturally express both nectin-1 and simian EGFR recognized by our anti-EGFR scFv. Biological titers in plaque forming units (PFU)/mL were determined by standard plaque assays on Vero cells, and physical titers in genome copies (gc)/mL were established by quantitative real-time PCR for the HSV-1 early gene U_L5 encoding a DNA helicase-primase subunit.

The entry-receptor specificities of the four viruses were verified by infection of cells expressing either no gD receptor (B78H1), human nectin-1 (B78-C),[16] or EGFRvIII (B78-vIII). Images of mCherry

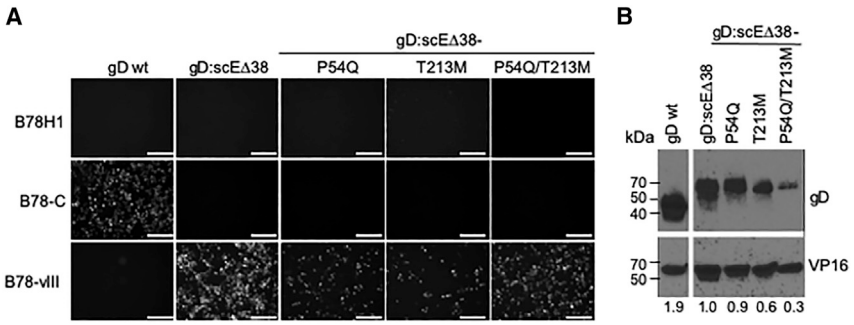

Figure 4. Virus Entry Specificities and gD Abundance in Virions

(A) Viruses produced by BAC DNA transfection of Vero cells were used to infect B78-H1, B78-C (nectin-1$^+$), and B78-vIII (EGFRvIII$^+$) cells for 20 h. Viruses are identified at the top of the columns according to their gD protein. Entry was recorded as mCherry fluorescence. Scale bars, 200 μm. (B) Western blots showing gD and VP16 contents of purified virions. Relative gD band intensities normalized to VP16 and set to gD:scEΔ38 = 1× are shown below the lanes.

expression from the common backbone of these viruses at 20 h post-infection showed that none of the retargeted viruses was able to enter into B78H1 or B78-C cells, while all could enter into B78-vIII cells, confirming that entry was strictly dependent on cellular expression of primate EGFR (Figure 4A). In contrast, a control virus expressing WT gD from the same backbone was able to enter B78-C cells but not B78H1 or B78-vIII cells.

mar Mutations Reduce Retargeted gD Incorporation into Virus Particles

We assessed retargeted gD representation in purified virions by western blot analysis using DL6 as the primary antibody. To control for differences in loaded particle numbers and contents, we also probed the blots with antibodies to the tegument protein VP16. As exemplified by the results presented in Figure 4B, retargeting reduced gD incorporation relative to VP16 and the *mar* mutations, particularly when combined, enhanced this effect. These results indicated that both retargeting and the *mar* mutations can limit the abundance of gD in mature virions, most likely a result of impaired intracellular processing of the modified proteins, reduced stability, or both. We have not observed similar differences in gB/VP16 ratios among this set of viruses.

mar Mutations Increase Resistance to Virus Neutralization by mAbs

We performed neutralization assays to determine the sensitivity of the retargeted virus and its mutant counterparts to inactivation by mAbs MC5 and MC23. Vero cells were infected with mixtures of virus and serial dilutions of MC5 or MC23, overlaid with high-density medium, and plaques were counted 48 h later. Figure 5 shows that the retargeted virus was sensitive to neutralization by both mAbs and that each *mar* mutation increased the resistance of the retargeted virus in a manner consistent with the earlier binding and fusion-inhibition results. Specifically, the P54Q mutant showed resistance to mAb MC5, and the T213M mutant was resistant to MC23 (Figure 5A). Furthermore, the P54Q/T213M double mutant was resistant to both mAbs (Figure 5B).

Based on the SPRi results, we might expect that antigenic sites mutated to block recognition by one member of a mAb community would no longer be efficiently recognized by other members of the same community, which would suggest that a single *mar* mutation may be sufficient to block gD recognition by multiple VN antibodies. We examined this possibility by testing the resistance of the double mutant retargeted virus to VN by two other mAbs, H162 from the same group as MC5 (blue), and LP2 from the same group as MC23 (red). H162 neutralized the retargeted virus, while the double mutant was fully protected (Figure 6A). The double mutant also showed increased resistance to LP2, although some remaining sensitivity was evident at the higher mAb concentrations (Figure 6B). These data were consistent with the SPRi data demonstrating that H162 binding to retargeted gD was abolished by the double mutation, while LP2 showed low residual binding to the double mutant retargeted gD (Figure 2D). Thus, the effects of the mutations on virus neutralization were not limited to a single representative each of the blue and red mAb groups.

DISCUSSION

We and others have previously demonstrated that oHSV retargeting can be a safe and effective strategy to achieve selective infection and lysis of tumor cells following intratumoral vector delivery.[17] Retargeting ligands have included scFv specific for receptors that are prominently expressed on tumor cells, including human EGFR/EGFRvIII,[5] epithelial cell adhesion molecule (EpCAM),[18] and human epidermal growth factor receptor 2 (HER2).[19] Full retargeting requires modifications of the major entry receptor-binding envelope glycoprotein, gD, to prevent recognition of the viral cognate receptors and enable virus attachment/entry through a new receptor. Systemically delivered retargeted oHSV has been shown to accumulate in flank tumors in nude mice,[5] and scFvs can be humanized to minimize an immune response to the novel ligand. However, systemic injection in HSV-immune patients will likely result in oHSV neutralization in the bloodstream, thereby blocking infection of tumors.

HSV is readily neutralized by antibodies that recognize different epitopes in envelope glycoproteins, most prominently gD and gB involved in attachment and entry.[8,12] Since retargeting changes the structure of gD, we first sought to determine its impact on the epitope landscape of gD. Using SPRi, we compared the purified ectodomain of retargeted gD to that of WT gD for binding by a broad panel of mAbs that have well-defined recognition sites on WT gD, including epitopes that co-localize with sites required for binding to the gD

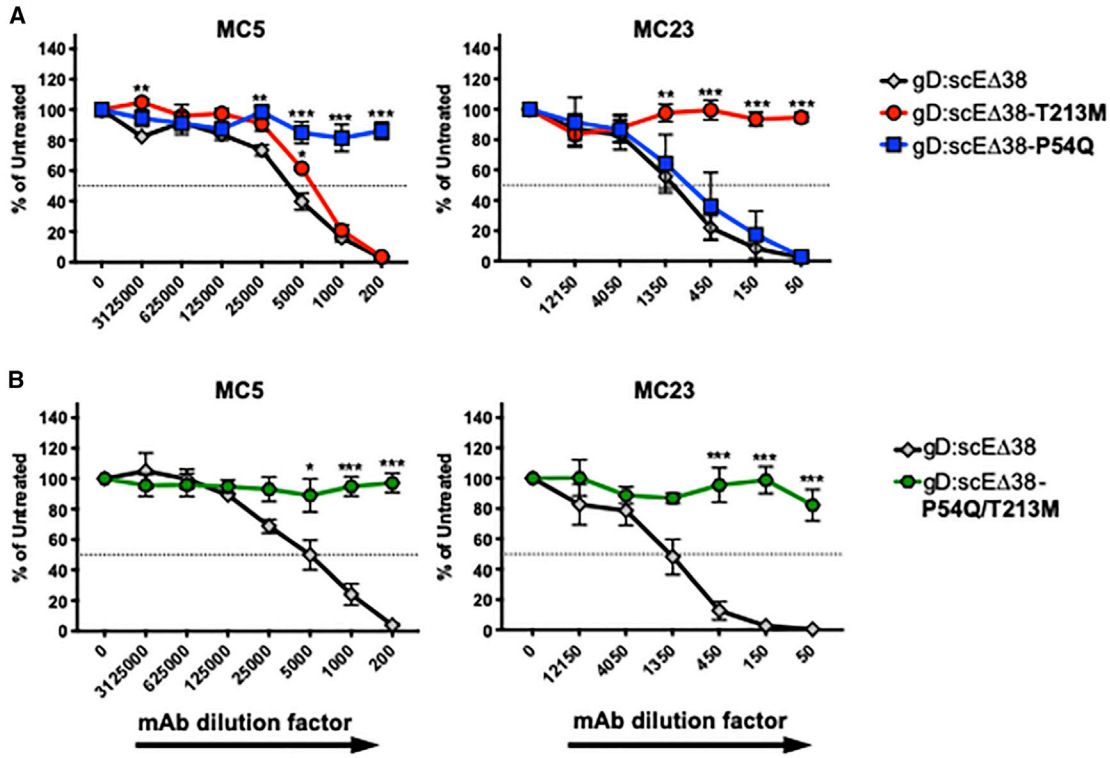

Figure 5. Neutralization of Retargeted Viruses by mAbs MC5 and MC23

KNTc viruses named to the right of the panels according to their gD gene were incubated with VN mAbs MC5 (left) or MC23 (right) at a range of dilutions (x axis) prior to infection of Vero cells. Infected cell monolayers were overlaid with high-density medium, and plaques were counted 48 h later. Representative results show the percentage PFU relative to virus-only control wells (100%). (A) Neutralization of retargeted gD virus (gD:scEΔ38) and single-*mar* mutant derivatives. (B) Retargeted gD virus and its double-*mar* mutant derivative. Data represent the averages ± SEM of three independent experiments using triplicate wells each. Statistically significant differences between each gD mutant virus and the parental retargeted virus at each mAb dilution were determined by two-way ANOVA (*$p < 0.01$, **$p < 0.001$, ***$p < 0.0001$).

cognate receptors.[11] As expected, the deletion of gD residues 2–24 in retargeted gD, designed to eliminate HVEM binding,[5] abolished the binding by antibodies of the yellow community that recognize N-terminal residues of WT gD (Figure 2). We also observed reduced binding of the neutralizing mAbs within the green, red, and blue groups, except H162 (blue), and increased binding of those mAbs in the brown group that recognize linear epitopes near the C terminus of the gD ectodomain. Thus, elimination of residues involved in gD receptor binding, along with insertion of a foreign ligand, blocked mAb binding to the directly affected epitopes and reduced or increased the exposure of epitopes in other parts of the molecule to various degrees.

Based on these results, we examined the effects of previously identified *mar* mutations, P54Q and T213M, that block HSV neutralization by mAbs MC5 and MC23, respectively,[13,14] representing the blue and red groups. We found that these mutations not only blocked retargeted gD binding by these specific mAbs, but also significantly reduced or eliminated the binding by other members of the same groups. These results were not unexpected since the tested mAbs were grouped by their abilities to compete mutually or semi-mutually for gD binding,[11] indicating overlapping epitopes. We then asked whether combining these mutations would have an additive or potentially synergistic effect or, conversely, might restore the binding of certain mAbs. Importantly, the double-mutant retargeted gD appeared to combine the specific and global effects of the two mutations, providing encouragement that a multi-site mutational strategy might translate to viral resistance to neutralizing antibodies in patient immune sera.

We constructed mutant viruses to determine whether the pattern of VN mirrored these assessments of isolated gD recognition. The mutant retargeted viruses, supported by the entry-enhancing activity of gB:NT, were viable and resistant to neutralization by either or both MC5 and MC23 as well as other neutralizing antibodies from the same mAb groups, consistent with the antibody recognition assays. However, we observed reduced virion incorporation, particularly of the double mutant retargeted gD, consistent with reduced stability, aberrant intracellular processing and trafficking, or both. Thus, the utility of these viruses depends on the relative impact of reduced gD representation in virions on infectivity versus increased resistance to VN antibodies. It remains largely unknown how much gD is required for effective infection. It has been reported that a 500-fold reduction in gD expression levels does not noticeably reduce HSV entry into keratinocytes, although it reduces cell-to-cell spread by a

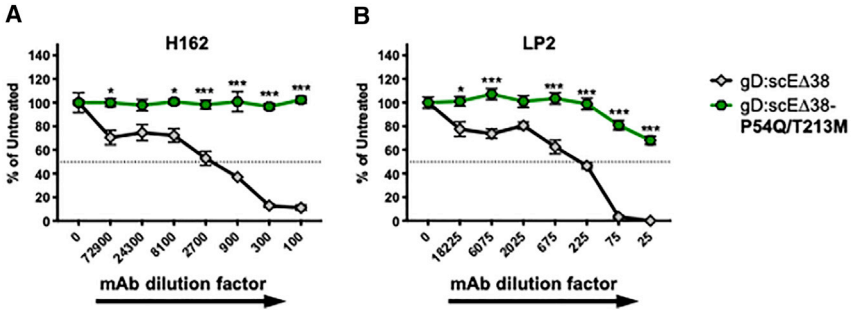

Figure 6. Retargeted and Double-*mar* Mutant Retargeted Virus Neutralization

Viruses were incubated with a range of mAb dilutions (x axis) prior to infection of Vero cells. Infected cell monolayers were overlaid with high-density medium, and plaques were counted 48 h later. Representative results show the percentage PFU relative to virus-only control wells (100%). (A) mAb LP2; (B) mAb H162. Data are shown as the averages of triplicate wells ± SEM. Statistically significant differences between the retargeted gD double mutant virus and the parental retargeted virus at each mAb dilution were determined by two-way ANOVA (*$p < 0.01$, **$p < 0.001$, ***$p < 0.0001$).

factor of 10, but entry and spread in other cell types, including Vero, can be severely impaired.[20] The authors proposed that the relatively high levels of nectin-1 on the surface of keratinocytes might compensate for the low abundance of gD. In another study, Zhou and Roizman[21] reported productive infection by a fully retargeted recombinant virus despite undetectable levels of its retargeted gD. Tumors often overexpress growth factor receptors, such as EGFR, HER2, MET, and others, suggesting that low gD levels in retargeted virions may increase the virus specificity for tumor cells if indeed high receptor abundance is required for infection. However, it has also been reported that low levels of gD increase HSV sensitivity to neutralizing antibodies.[20] Our current work aims at exploring these issues, in part by addressing the suspected processing defects of retargeted gD mutants. We anticipate that a favorable balance can be found between reduced expression of retargeted gD due to *mar* mutations and increased virus resistance to VN antibodies mediated by the same mutations. Our initial study presented herein is encouraging in that it provides evidence that different epitope changes can be combined to protect retargeted virus from inactivation by several mAbs representative of VN activity in human immune sera.

MATERIALS AND METHODS

Plasmids

pENTR-Based Plasmids for Viral Genome Modification

pENTR-gD:scEΔ38. The previously described plasmid pgD:Δ224/38C-scEGFR[5] contains the anti-EGFR scFv between positions 1 and 25 of gD, a point mutation at position 38 causing a tyrosine-to-cysteine substitution (Y38C), and a unique BstBI site created by silent mutations at positions V34 (GTC to GTT), R35 (CGG to CGA), and R36 (CGC to AGA). The Y38C codon was deleted from this plasmid to generate pgD:scEΔ38 by replacement of the internal BstBI-BspEI fragment (BspEI at gD codons 88–90) with a BstBI-BspEI-digested PCR fragment amplified from pgD:Δ224/38C-scEGFR with primers hu91 and hu4 (Table S1) (H. Uchida and J.B.C., unpublished data). The resulting gD:scEΔ38 sequence was then transferred to pENTR1A by PCR amplification with primers gDatg-5′ and gDstop-3′ (Table S1) and blunt end cloning between the Gateway (GW)-compatible *att*L sites of plasmid pENTR1A at the DraI and EcoRV sites. The desired orientation of the insert (*att*L1-(5′-gD:scEΔ38-3′)-*att*L2) was identified by restriction analysis of recombinants and confirmed by DNA sequencing.

pENTR-gD:scEΔ38-P54Q was created by replacing the BstBI-BspEI fragment of pENTR-gD:scEΔ38 with a corresponding synthetic DNA fragment (GenScript, Piscataway, NJ, USA) specifying the codon P54Q change from CCG to CAG.

pENTR-gD:scEΔ38-T213M was created by cloning a synthetic DNA fragment (GenScript) encompassing the gD nucleotide sequence from the FspI site at gD codons 195–197 to the KasI site at codons 286–288 and specifying the codon T213M change (ACG to ATG) between the FspI and KasI sites of pENTR-gD:scEΔ38.

pENTR-gD:scEΔ38-P54Q/T213M was created by replacing the WT FspI-KasI fragment of pENTR-gD:scEΔ38-P54Q with the synthetic T213M mutant fragment.

pVT-Bac-Based Plasmids for gD Ectodomain Expression in Insect Cells

The coding sequences for the mature ectodomains (truncated after gD residue 306) of WT, retargeted, and mutant retargeted gDs were isolated by PCR amplification with primers pVTBac gD:scEGFRΔ38-5′ and pVTBac gD:scEGFRΔ38-3′ specified in Table S1 using the respective pENTR recombinants described above as template. Each PCR product was cloned into baculovirus expression plasmid pVT-Bac (kindly provided by Thierry Vernet, Biotechnology Research Institute, Montreal, QC, Canada), essentially as described[22] but using NotI instead of PstI at the 3′ end of the insert and omitting the C-terminal His tag.

pcDNA3.1-Based Plasmids for gD Expression in Mammalian Cells

The coding sequences for WT, retargeted, and retargeted mutant gDs were cloned into a pcDNA3.1 derivative containing a GW recombination cassette between the cytomegalovirus (CMV) promoter and bGH polyadenylation region[23] by LR Clonase II (Thermo Fisher Scientific, Waltham, MA, USA)-mediated recombination with the respective pENTR-based plasmids.

Other Plasmids

gB:NT expression plasmid pCAgB:NT was as described.[24] gH and gL expression plasmids pPEP100 and pPEP101, respectively, were kindly provided by Patricia Spear (Northwestern University).[25]

pCX4-bsr-DEST, pCL-gag-pol, and pHCMV-VSVG were kind gifts from Akihiro Umezawa (NRICHD, Tokyo, Japan). PT3.5/CMV-EGFRvIII[26] was a gift from John Ohlfest (Addgene, plasmid # 20280). Plasmids $RLuc8_{1-7}$ and $RLuc8_{8-11}$ were described previously.[15,27]

pCX4-bsr-EGFRvIII was constructed by PCR amplification of the EGFRvIII coding sequence from plasmid PT3.5/CMV-EGFRvIII with primers Sal1EGFRvIIIF and Xho1EGFRvIIIR (Table S1), cloning of the SalI-XhoI-digested product between the SalI and XhoI sites of pENTR1A, and LR Clonase II-mediated recombination with pCX4-bsr-DEST.

pUL5 was constructed by PCR amplification of the U_L5 coding sequence with primers UL5F and UL5R (Table S1) on KOS-37 BAC[28] DNA, and cloning of the product into pCR-Blunt II-TOPO using the Zero Blunt TOPO PCR cloning kit (Thermo Fisher Scientific).

All new constructs were confirmed by DNA sequencing.

Viruses

A GW-compatible gD null viral backbone, KNTc-ΔgD:GW (Figure 1B), on a bacterial artificial chromosome (BAC) was derived from KNTc BAC[29] by Red-mediated replacement of the gD coding sequence with a GW cassette, GW-Zeo, amplified with primers targeting the proximal 5′ and 3′ gD untranslated sequences, essentially as described.[29] WT and retargeted gD genes were then introduced by LR Clonase II-mediated recombination of the GW cassette with the different pENTR-based gD plasmids. Infectious viruses were produced by transfection of Vero cells, and biological titers were determined by standard plaque assays on Vero cells.

All recombinant viruses were confirmed by DNA sequencing across the gD cassettes.

Cells

Murine melanoma B78H1, B78-C10 (nectin-1-transduced B78H1),[30] and B78-C cells (nectin-1-transduced B78H1)[16] were cultured in Dulbecco's modified Eagle's medium (DMEM; Thermo Fisher Scientific) supplemented with 5% fetal bovine serum (FBS; Sigma-Aldrich, St. Louis, MO, USA). African green monkey kidney Vero cells (ATCC CCL-81) were cultured in DMEM supplemented with 5% FBS. B78-vIII cells were established by infection of B78H1 cells with a recombinant retrovirus expressing EGFRvIII, produced by co-transfection of 293T cells (ATCC CRL-3216) with plasmids pCX4-bsr-EGFRvIII, pCL-gag-pol, and pHCMV-VSVG. Infected B78H1 cultures were selected for resistance to blasticidin (10 μg/mL), and resistant pools were tested for EGFRvIII expression by western blots and flow cytometry analysis with anti-EGFR mAb H11 (Thermo Fisher Scientific). After validation, the cells were sorted at the Cell Sorting Facility of the University of Pittsburgh McGowan Institute based on expression levels, and clones were isolated from a high-expressing fraction by limiting dilution. Clone 11B was used in the current study (Figure S1).

gD Ectodomain Production and mAb Binding (SPRi) Assays

All soluble proteins used in this study were produced in baculovirus-infected insect (Sf9) cells and purified using a DL6 immunosorbent column, as described previously.[22,31,32]

Analysis of gD mAb binding was performed using soluble proteins on the Carterra CFM/SPRi system as described previously.[11,33,34] CFM-2 was used to create a 48-spot microarray of amine-coupled mAbs on a CDM200M sensor chip (Xantec, Düsseldorf, Germany). Upon docking the printer chip into the SPR imager (IBIS MX96, IBIS Technologies, Enschede, the Netherlands), the chip was blocked with ethanolamine and the system primed with a running buffer of PBS-0.01% Tween 20. mAb binding was assessed by flowing 100 nM soluble gD across the printed mAb array; 1 M glycine (pH 2.0) was used for regeneration.

Fusion Assays

The fusion assay was described previously.[15,35,36] Briefly, 5×10^4 B78HI cells (effector cells) were seeded on white, cell culture-treated 96-well plates. 4×10^5 B78-vIII cells (target cells) were seeded on six-well plates. Transfections were performed the following day. A master mix containing 375 ng of pCAgB:NT and 125 ng of each of the indicated pcDNA3.1-based gD constructs, pPEP100, pPEP101, and $Rluc8_{1-7}$, was split over three wells of effector cells. Target cells were transfected with 1 μg of $Rluc8_{8-11}$ plasmid per well. Forty-eight hours post-transfection, effector cells were pre-incubated for 1 h at 37°C with EnduRen substrate (Promega, Madison, WI, USA) diluted in fusion medium (DMEM without phenol red, with 50 mM HEPES and 5% FBS). Target cells were detached with Gibco Versene solution (Thermo Fisher Scientific), resuspended in fusion medium, and transferred to the effector cells. Fusion was triggered by the addition of target cells. A negative control (effector cells transfected without gD plasmid) was also included. Luciferase production was monitored during 6 h with measurements every hour using a BioTek plate reader.

Fusion Inhibition

Transfected effector cells were pre-incubated with both EnduRen substrate and serial, 2-fold dilutions of the indicated anti-gD mAbs (20–2.5 μg/mL or no mAb as control) in a final volume of 80 μL.[15,35,36]

gc Number Determination

Viral DNA was isolated using a blood and tissue DNA extraction kit (QIAGEN, Venlo, Netherlands). gc titers were calculated relative to a standard curve generated for each experiment using a 10-fold dilution series of plasmid pUL5 (corresponding to 3×10^6 to 3×10^2 copies of the HSV genome) and a custom FAM-MGB TaqMan primer probe set (UL5qPCR-F, UL5qPCR-R, UL5 MGB probe, Table S1; Thermo Fisher Scientific); the amplification efficiency of plasmid-based U_L5 was 98%–100%. Samples, standard curve, and negative controls

were run together in triplicate in MicroAmp optical 96-well reaction plates with the StepOne Plus real-time PCR system (Applied Biosystems). Reaction mixtures were as follows: 2 μL of DNA, 1 μL of the 20× UL5 FAM-MGB TaqMan primer probe set, and 10 μL of TaqMan Fast advanced universal PCR master mix (2×) in a total PCR volume of 20 μL. Amplification conditions were as follows: 2 min at 50°C and 20 s at 95°C for the first cycle, followed by 40 cycles of 95°C for 1 s and 60°C for 20 s.

Entry Assay

Cells were infected overnight with 2,500 gc/cell and imaged for mCherry expression under a Nikon Diaphot fluorescence microscope (Nikon, Melville, NY, USA) with MetaMorph imaging software (Molecular Devices, San Jose, CA, USA).

Western Blots

Equal gc numbers of purified virus stocks were denatured by boiling in Laemmli sample buffer with 2-mercaptoethanol (Bio-Rad, Hercules, CA, USA) and electrophoresed on precast 4%–15% SDS-PAGE gels (Bio-Rad). Proteins were transferred to polyvinylidene fluoride (PVDF) membranes (Millipore, Billerica, MA, USA) and reacted with anti-gD (DL6, Santa Cruz Biotechnology, Dallas, TX, USA) or anti-VP16 (Santa Cruz Biotechnology) antibody prior to incubation with horseradish peroxidase (HRP)-conjugated rabbit anti-mouse immunoglobulin G (IgG; Abcam, Cambridge, UK). Membranes were developed with ECL (enhanced chemiluminescence) Plus (Thermo Fisher Scientific). Signal intensities were measured with ImageJ software.[37]

For screening of the B78-vIII clones, 10^7 cells of each clone were collected and lysed in 1 mL of 1× radioimmunoprecipitation assay (RIPA) buffer (Thermo Fisher Scientific). Protein denaturation, electrophoresis, and transfer to PVDF membranes were as above. Membranes were sequentially reacted with anti-EGFR monoclonal antibody H11 (Thermo Fisher Scientific) and HRP-conjugated rabbit anti-mouse IgG (Abcam, Cambridge, UK) and developed with ECL Plus.

Virus Neutralization

Vero cells were seeded at 2.5×10^4 cells per well in a 48-well tissue culture plate 24 h prior to infection. Purified viruses (50–75 PFU) were mixed with mAbs at a range of dilutions in serum-free medium and the mAb/virus mixtures were used to infect Vero cell monolayers for 1.5 h at 37°C prior to the addition of high-density medium. Plaques were counted 48 h later under the Nikon Diaphot fluorescence microscope.

Statistical Analysis

GraphPad Prism 8 software for MacOS was used for all statistical analyses. Averages for each experiment are shown ±SEM. As noted in the relevant figure legends, one-way or two-way ANOVAs were used to determine the statistical significance of differences observed between groups, and significant differences are indicated in the figures ($^*p < 0.01$, $^{**}p < 0.001$, $^{***}p < 0.0001$) or, for Figure 3, described in the legend.

SUPPLEMENTAL INFORMATION

Supplemental Information can be found online at https://doi.org/10.1016/j.omtm.2019.12.013.

AUTHOR CONTRIBUTIONS

Conception and Design: J.C.G., G.H.C., C.T., T.M.C., D.A., B.L.H., and J.B.C.; Methodology: all authors; Data Acquisition: C.T., T.M.C., D.A., H.L., and W.T.S.; Data Analysis and Interpretation: C.T., T.M.C., D.A., B.L.H., J.B.C., G.H.C., and J.C.G.; Manuscript Preparation: C.T., B.L.H., J.B.C., and J.C.G.; Manuscript Reviewing: T.M.C., D.A., and G.H.C.

CONFLICTS OF INTEREST

J.B.C. and J.C.G. are inventors of intellectual property licensed to Oncorus, Inc. (Cambridge, MA, USA). J.C.G. is a consultant and Chair of the Scientific Advisory Board of Oncorus, Inc. The remaining authors declare no competing interests.

ACKNOWLEDGMENTS

This study was supported by a CTSA SPIRiT Consortium pilot grant to J.C.G. and G.H.C., an Alliance for Cancer Gene Therapy (ACGT, United States) 2018 Investigator's Award in Cell and Gene Therapy for Cancer Research grant to J.C.G., and by National Institutes of Health (NIH, United States) grant R01-AI-18289-38 to G.H.C.

REFERENCES

1. Andtbacka, R.H., Kaufman, H.L., Collichio, F., Amatruda, T., Senzer, N., Chesney, J., Delman, K.A., Spitler, L.E., Puzanov, I., Agarwala, S.S., et al. (2015). Talimogene laherparepvec improves durable response rate in patients with advanced melanoma. J. Clin. Oncol. *33*, 2780–2788.

2. Pol, J., Kroemer, G., and Galluzzi, L. (2015). First oncolytic virus approved for melanoma immunotherapy. OncoImmunology *5*, e1115641.

3. Atanasiu, D., Saw, W.T., Eisenberg, R.J., and Cohen, G.H. (2016). Regulation of herpes simplex virus glycoprotein-induced cascade of events governing cell-cell fusion. J. Virol. *90*, 10535–10544.

4. Fontana, J., Atanasiu, D., Saw, W.T., Gallagher, J.R., Cox, R.G., Whitbeck, J.C., Brown, L.M., Eisenberg, R.J., and Cohen, G.H. (2017). The fusion loops of the initial prefusion conformation of herpes simplex virus 1 fusion protein point toward the membrane. MBio *8*, e01268-14.

5. Uchida, H., Marzulli, M., Nakano, K., Goins, W.F., Chan, J., Hong, C.S., Mazzacurati, L., Yoo, J.Y., Haseley, A., Nakashima, H., et al. (2013). Effective treatment of an orthotopic xenograft model of human glioblastoma using an EGFR-retargeted oncolytic herpes simplex virus. Mol. Ther. *21*, 561–569.

6. Uchida, H., Chan, J., Goins, W.F., Grandi, P., Kumagai, I., Cohen, J.B., and Glorioso, J.C. (2010). A double mutation in glycoprotein gB compensates for ineffective gD-dependent initiation of herpes simplex virus type 1 infection. J. Virol. *84*, 12200–12209.

7. Uchida, H., Hamada, H., Nakano, K., Kwon, H., Tahara, H., Cohen, J.B., and Glorioso, J.C. (2018). Oncolytic herpes simplex virus vectors fully retargeted to tumor-associated antigens. Curr. Cancer Drug Targets *18*, 162–170.

8. Cairns, T.M., Huang, Z.Y., Gallagher, J.R., Lin, Y., Lou, H., Whitbeck, J.C., Wald, A., Cohen, G.H., and Eisenberg, R.J. (2015). Patient-specific neutralizing antibody responses to herpes simplex virus are attributed to epitopes on gD, gB, or both and can be type specific. J. Virol. *89*, 9213–9231.

9. Cairns, T.M., Huang, Z.Y., Whitbeck, J.C., Ponce de Leon, M., Lou, H., Wald, A., Krummenacher, C., Eisenberg, R.J., and Cohen, G.H. (2014). Dissection of the antibody response against herpes simplex virus glycoproteins in naturally infected humans. J. Virol. *88*, 12612–12622.

10. Holland, T.C., Marlin, S.D., Levine, M., and Glorioso, J. (1983). Antigenic variants of herpes simplex virus selected with glycoprotein-specific monoclonal antibodies. J. Virol. *45*, 672–682.

11. Cairns, T.M., Ditto, N.T., Lou, H., Brooks, B.D., Atanasiu, D., Eisenberg, R.J., and Cohen, G.H. (2017). Global sensing of the antigenic structure of herpes simplex virus gD using high-throughput array-based SPR imaging. PLoS Pathog. *13*, e1006430.

12. Cairns, T.M., Fontana, J., Huang, Z.Y., Whitbeck, J.C., Atanasiu, D., Rao, S., Shelly, S.S., Lou, H., Ponce de Leon, M., Steven, A.C., et al. (2014). Mechanism of neutralization of herpes simplex virus by antibodies directed at the fusion domain of glycoprotein B. J. Virol. *88*, 2677–2689.

13. Lazear, E., Whitbeck, J.C., Ponce-de-Leon, M., Cairns, T.M., Willis, S.H., Zuo, Y., Krummenacher, C., Cohen, G.H., and Eisenberg, R.J. (2012). Antibody-induced conformational changes in herpes simplex virus glycoprotein gD reveal new targets for virus neutralization. J. Virol. *86*, 1563–1576.

14. Atanasiu, D., Saw, W.T., Lazear, E., Whitbeck, J.C., Cairns, T.M., Lou, H., Eisenberg, R.J., and Cohen, G.H. (2018). Using antibodies and mutants to localize the presumptive gH/gL binding site on herpes simplex virus gD. J. Virol. *92*, e01694-18.

15. Atanasiu, D., Saw, W.T., Gallagher, J.R., Hannah, B.P., Matsuda, Z., Whitbeck, J.C., Cohen, G.H., and Eisenberg, R.J. (2013). Dual split protein-based fusion assay reveals that mutations to herpes simplex virus (HSV) glycoprotein gB alter the kinetics of cell-cell fusion induced by HSV entry glycoproteins. J. Virol. *87*, 11332–11345.

16. Uchida, H., Shah, W.A., Ozuer, A., Frampton, A.R., Jr., Goins, W.F., Grandi, P., Cohen, J.B., and Glorioso, J.C. (2009). Generation of herpesvirus entry mediator (HVEM)-restricted herpes simplex virus type 1 mutant viruses: resistance of HVEM-expressing cells and identification of mutations that rescue nectin-1 recognition. J. Virol. *83*, 2951–2961.

17. Campadelli-Fiume, G., Petrovic, B., Leoni, V., Gianni, T., Avitabile, E., Casiraghi, C., and Gatta, V. (2016). Retargeting strategies for oncolytic herpes simplex viruses. Viruses *8*, 63.

18. Shibata, T., Uchida, H., Shiroyama, T., Okubo, Y., Suzuki, T., Ikeda, H., Yamaguchi, M., Miyagawa, Y., Fukuhara, T., Cohen, J.B., et al. (2016). Development of an oncolytic HSV vector fully retargeted specifically to cellular EpCAM for virus entry and cell-to-cell spread. Gene Ther. *23*, 479–488.

19. Menotti, L., Cerretani, A., Hengel, H., and Campadelli-Fiume, G. (2008). Construction of a fully retargeted herpes simplex virus 1 recombinant capable of entering cells solely via human epidermal growth factor receptor 2. J. Virol. *82*, 10153–10161.

20. Huber, M.T., Wisner, T.W., Hegde, N.R., Goldsmith, K.A., Rauch, D.A., Roller, R.J., Krummenacher, C., Eisenberg, R.J., Cohen, G.H., and Johnson, D.C. (2001). Herpes simplex virus with highly reduced gD levels can efficiently enter and spread between human keratinocytes. J. Virol. *75*, 10309–10318.

21. Zhou, G., and Roizman, B. (2006). Construction and properties of a herpes simplex virus 1 designed to enter cells solely via the IL-13α2 receptor. Proc. Natl. Acad. Sci. USA *103*, 5508–5513.

22. Sisk, W.P., Bradley, J.D., Leipold, R.J., Stoltzfus, A.M., Ponce de Leon, M., Hilf, M., Peng, C., Cohen, G.H., and Eisenberg, R.J. (1994). High-level expression and purification of secreted forms of herpes simplex virus type 1 glycoprotein gD synthesized by baculovirus-infected insect cells. J. Virol. *68*, 766–775.

23. Reinhart, B., Goins, W.F., Harel, A., Chaudhry, S., Goss, J.R., Yoshimura, N., de Groat, W.C., Cohen, J.B., and Glorioso, J.C. (2016). An HSV-based library screen identifies PP1α as a negative TRPV1 regulator with analgesic activity in models of pain. Mol. Ther. Methods Clin. Dev. *3*, 16040.

24. Uchida, H., Chan, J., Shrivastava, I., Reinhart, B., Grandi, P., Glorioso, J.C., and Cohen, J.B. (2013). Novel mutations in gB and gH circumvent the requirement for known gD receptors in herpes simplex virus 1 entry and cell-to-cell spread. J. Virol. *87*, 1430–1442.

25. Pertel, P.E., Fridberg, A., Parish, M.L., and Spear, P.G. (2001). Cell fusion induced by herpes simplex virus glycoproteins gB, gD, and gH-gL requires a gD receptor but not necessarily heparan sulfate. Virology *279*, 313–324.

26. Wiesner, S.M., Decker, S.A., Larson, J.D., Ericson, K., Forster, C., Gallardo, J.L., Long, C., Demorest, Z.L., Zamora, E.A., Low, W.C., et al. (2009). De novo induction of genetically engineered brain tumors in mice using plasmid DNA. Cancer Res. *69*, 431–439.

27. Ishikawa, H., Meng, F., Kondo, N., Iwamoto, A., and Matsuda, Z. (2012). Generation of a dual-functional split-reporter protein for monitoring membrane fusion using self-associating split GFP. Protein Eng. Des. Sel. *25*, 813–820.

28. Gierasch, W.W., Zimmerman, D.L., Ward, S.L., Vanheyningen, T.K., Romine, J.D., and Leib, D.A. (2006). Construction and characterization of bacterial artificial chromosomes containing HSV-1 strains 17 and KOS. J. Virol. Methods *135*, 197–206.

29. Miyagawa, Y., Marino, P., Verlengia, G., Uchida, H., Goins, W.F., Yokota, S., Geller, D.A., Yoshida, O., Mester, J., Cohen, J.B., and Glorioso, J.C. (2015). Herpes simplex viral-vector design for efficient transduction of nonneuronal cells without cytotoxicity. Proc. Natl. Acad. Sci. USA *112*, E1632–E1641.

30. Miller, C.G., Krummenacher, C., Eisenberg, R.J., Cohen, G.H., and Fraser, N.W. (2001). Development of a syngenic murine B16 cell line-derived melanoma susceptible to destruction by neuroattenuated HSV-1. Mol Ther. *3*, 160–168.

31. Lazear, E., Carfi, A., Whitbeck, J.C., Cairns, T.M., Krummenacher, C., Cohen, G.H., and Eisenberg, R.J. (2008). Engineered disulfide bonds in herpes simplex virus type 1 gD separate receptor binding from fusion initiation and viral entry. J. Virol. *82*, 700–709.

32. Nicola, A.V., Willis, S.H., Naidoo, N.N., Eisenberg, R.J., and Cohen, G.H. (1996). Structure-function analysis of soluble forms of herpes simplex virus glycoprotein D. J. Virol. *70*, 3815–3822.

33. Abdiche, Y.N., Harriman, R., Deng, X., Yeung, Y.A., Miles, A., Morishige, W., Boustany, L., Zhu, L., Izquierdo, S.M., and Harriman, W. (2016). Assessing kinetic and epitopic diversity across orthogonal monoclonal antibody generation platforms. MAbs *8*, 264–277.

34. Abdiche, Y.N., Miles, A., Eckman, J., Foletti, D., Van Blarcom, T.J., Yeung, Y.A., Pons, J., and Rajpal, A. (2014). High-throughput epitope binning assays on label-free array-based biosensors can yield exquisite epitope discrimination that facilitates the selection of monoclonal antibodies with functional activity. PLoS ONE *9*, e92451.

35. Saw, W.T., Matsuda, Z., Eisenberg, R.J., Cohen, G.H., and Atanasiu, D. (2015). Using a split luciferase assay (SLA) to measure the kinetics of cell-cell fusion mediated by herpes simplex virus glycoproteins. Methods *90*, 68–75.

36. Nakane, S., and Matsuda, Z. (2015). Dual split protein (DSP) assay to monitor cell-cell membrane fusion. Methods Mol. Biol. *1313*, 229–236.

37. Rueden, C.T., Schindelin, J., Hiner, M.C., DeZonia, B.E., Walter, A.E., Arena, E.T., and Eliceiri, K.W. (2017). ImageJ2: ImageJ for the next generation of scientific image data. BMC Bioinformatics *18*, 529.